JOURNAL OF SOLID STATE CHEMISTRY 72, 2–13 (1988)

# The Electrical Properties of $A_2[Ru_{2-x}A_x]O_{7-y}$ ($A$ = Pb or Bi) Pyrochlores as a Function of Composition and Temperature*

R. A. BEYERLEIN,** H. S. HOROWITZ,† AND J. M. LONGO§

*Exxon Research and Engineering Co., Route 22 East, Annandale, New Jersey 08801*

Received February 2, 1987

The variable stoichiometry pyrochlore compounds $A_2[Ru_{2-x}A_x]O_{7-y}$ ($A$ = Pb or Bi) exhibit high electrical conductivity with room temperature values ranging from 10 to 1000 (ohm-cm)$^{-1}$, dependent upon composition. For the lead-containing series, resistivity vs temperature data show that there is a smooth variation from a positive to a negative temperature coefficient of resistivity (TCR) as a function of increasing lead content. Substitution of ~20% of the ruthenium by lead results in a material with essentially temperature-independent resistivity. In the bismuth-containing series, the essentially zero TCR at zero substitution is made progressively more negative as the extent of bismuth substitution is increased. The electrical conductivity of these pyrochlore compounds is discussed in terms of electron transfer between large conducting segments consisting of connected networks of $RuO_6$ octahedra. It is postulated that the thermally activated conductivity behavior exhibited by the negative TCR materials is associated with the presence of thin barrier regions resulting from the introduction of Pb or Bi on the Ru site. Results of infrared absorption measurements showing active modes associated with Pb–O but not with Ru–O bonds support this picture. 

## Introduction

A series of mixed-metal oxides with the pyrochlore structure that has previously been reported (*1, 2*) can be described by the general formula

$$A_2[Ru_{2-x}A_x]O_{7-y},$$

where $0 < x \leq 1$ and $y = 0.5$ for $A$ = Pb, and $0 < x \leq 1$, $0 \leq y \leq 0.5$ for $A$ = Bi.

* Dedicated to John B. Goodenough.

** To whom correspondence should be addressed at present address: Amoco Oil Co., P.O. Box 400, Naperville, IL 60566.

† Present address: E. I. du Pont de Nemours & Co., Wilmington, DE 19898.

§ Present address: Exxon Production Research Co., Box 2189, Houston, TX 77001.

0022-4596/88 $3.00


These materials are characterized by high electronic conductivity and have been demonstrated to be effective electrocatalysts for both evolution and reduction of oxygen (*2, 3*). They have also been shown to catalyze the selective electrooxidation of certain organic molecules (*2, 4*). The high electrical conductivity of these pyrochlore compounds (10 to 1000 (ohm-cm)$^{-1}$ at room temperature) is essential to their high electrocatalytic activity.

The method of synthesis involves low-temperature reaction of the appropriate cations in an oxygenated, strongly alkaline solution (*1, 2*). The product obtained is a finely divided oxide that can be described by the general formula

$$A_2B_2O_6O',$$

where $A$ and $B$ represent the two cation sites in the pyrochlore structure. The pyrochlore structure can be viewed as two interpenetrating networks (*5*). The $B_2O_6$ sublattice is made up of a connected network of $BO_6$ octahedra which share only corners so as to form interconnected cage-like holes which, in turn, contain a cuprite-like network formed by the $A_2O'$ sublattice. The special oxygens, O′, located at the centers of the cages, may be partially or totally absent. It has been suggested that the high electrical conductivity found in the end members, $Pb_2Ru_2O_{6.5}$ (*6, 7*) and $Bi_2Ru_2O_7$ (*8*), might predominantly result from covalent interactions within the three-dimensional, corner-shared network of $RuO_6$ octahedra (*6, 8*).

The alkaline medium synthesis route (*1, 2*) allows substitution of up to 50% of the Ru cations on the $B$ site by Pb or Bi. The synthesis conditions together with previous materials characterization results (*1, 2*) indicate that the substitution is by $Pb^{4+}$ in the case of the lead ruthenates. The oxidation state of the $B$-site bismuth, in the case of the bismuth ruthenates, is not known. The resulting "expanded" pyrochlores show an increased cubic cell dimension with increased substitution of the larger post-transition cations for Ru (*1, 2*). All of these compounds exhibit high electrical conductivity. This paper describes the results of a detailed study of the electrical conductivity of these pyrochlore compounds as a function of composition, temperature, and state of crystallinity. The results indicate the ease of "tailoring" the temperature coefficient of resistivity (TCR) of these highly conductive pyrochlores while at the same time reducing their noble metal content. For the lead-containing series, resistivity vs temperature data show that there is a smooth variation from a positive to a negative temperature coefficient of resistivity as a function of increasing lead content. In the bismuth-containing series, the essentially zero TCR at zero substitution becomes progressively more negative with increasing bismuth content. In all cases increased substitution on the $B$ site results in a gradual decrease in conductivity.

## Experimental

### *1. Sample Preparation*

The compounds with no $B$-site substitution ($x = 0$) were prepared by conventional solid state synthesis at temperatures from 700 to 1000°C. The expanded pyrochlores with $x > 0$ were prepared by the low-temperature alkaline medium synthesis route previously described (*1, 2*). Measurements were performed both on samples prepared crystalline from solution and on samples prepared as "incipient" pyrochlores. Samples of the latter type were characterized by broad X-ray diffraction spectra. Crystallinity was developed in these predominantly amorphous samples by subsequent heat treatment at temperatures ranging from 350 to 500°C (*1*). Unless otherwise indicated discussion of resistivity measurements will refer to measurements made on samples with fully developed crystallinity. The limited temperature stability of the expanded pyrochlores with $x > 0$ (*1*) precluded the preparation of sintered samples, and the resistivity measurements were necessarily carried out on pressed powder samples. A summary of the materials used in these investigations, including a tabulation of the composition, preparation method, surface area, and lattice parameter, is given in Table I.

### *2. Resistivity Measurement Apparatus*

Four-probe dc conductivity measurements were performed on compacted powder samples using the apparatus shown

TABLE I

MATERIALS DATA FOR CRYSTALLINE EXPANDED PYROCHLORES, $A_2[Ru_{2-x}A_x]O_{7-y}$, $A$ = Pb OR Bi

| $A$ | Composition $x$ | Preparation method (Ref. (*1*)) | BET surface area ($m^2/g$) | Lattice parameter (Å) |
|---|---|---|---|---|
| Pb | 0 | Ceramic, 850°C in air | <1 | 10.252 |
| | 0.14 | Amorphous from solution, 600°C, 2 hr, air | 5 | 10.32 |
| | 0.31 | Amorphous from solution, 500°C, ON[a], air | 6 | 10.35 |
| | 0.41 | Crystalline from solution, 400°C, 2 hr, air | 51 | 10.38 |
| | 0.65 | Amorphous from solution, 400°C, 2 hr, air | 22 | 10.47 |
| | 0.77 | Amorphous from solution, 400°C, ON, air | 17 | 10.54 |
| | 0.84 | Amorphous from solution 400°C, ON, air | 9 | 10.57 |
| | 1.06 | Amorphous from solution, 350°C, ON, air | 13 | 10.61 |
| Bi | 0 | Ceramic prep | 0.2 | 10.30 |
| | 0.28 | Crystalline from solution, 400°C, ON, air | 33 | 10.36 |
| | 0.52 | Crystalline from solution, 100°C, ON, air | 42 | 10.41 |

[a] ON = overnight.

schematically in Fig. 1. The sectioned piston-in-cylinder conductivity cell (6.35 mm i.d.) in Fig. 2 is patterned after that described by Euler (*9*). The insulating sections of the cell were fabricated from the machinable ceramic, Mykroy (*10*). The

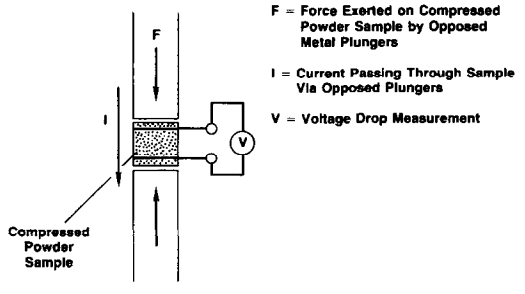


FIG. 1. Apparatus for performing four-probe dc conductivity measurements under dynamic load.

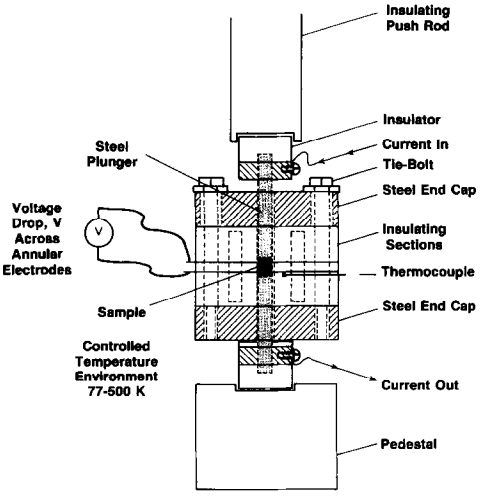


FIG. 2. The sectioned piston-in-cylinder conductivity cell.

conductivity cell was located in an internally supported, stainless-steel dewar so that measurements could be performed under dynamic load over a wide temperature range (77 to 480 K). Low temperatures were obtained using a liquid $N_2$ bath, while intermediate temperatures were produced by controlled heating using resistance heaters bonded to a Cu jacket which was in turn fixed to the metal-supporting sections of the cell. This Cu heating jacket also served to minimize axial temperature gradients in the conductivity cell. The sample was kept under dynamic load (typically 110 MPa applied uniaxial stress) in order to ensure good electrical contact and to eliminate possible systematic errors produced by a change in sample compression as the temperature was changed.

Typical measuring currents were 100 mA; the voltage drop across the pair of annular Cu electrodes, which were spaced 3.18 mm apart, was measured using a resolution of 1 $\mu$V.

### 3. *Measurement Procedure*

During a typical run, the sample resistivity ($\rho$) was measured at about 10°C intervals during controlled warm-up of the cell. Use of appropriate averages of voltage drop signals measured in forward and reverse polarity and in forward and reverse current directions allowed elimination of the effect of spurious emfs and of small axial temperature gradients in the conductivity cell. The effective density of the compacted powder samples was typically about 70% of theoretical density for the nonexpanded ($x = 0$) materials and about 50% of theoretical density for the expanded pyrochlores. The resistivity of each sample was determined from the geometry described without any correction for density.

It was found that reproducibility of $\rho$ vs $T$ to 2% could be ensured by precompaction and *in situ* drying of the powder sample prior to cooling it in the compression cell. This was achieved by load cycling at room temperature several times and then heating to about 200°C under load and maintaining that temperature for at least 1 h before cooling the cell to liquid nitrogen temperature under constant load. A dry atmosphere was maintained by blowing dry $N_2$ gas into the sample chamber throughout the course of a measurement. Otherwise, moisture pick-up by the sample ($\frac{1}{2}$ to 1 wt%) resulted in a 1 to 5% increase in the measured resistivity.

Increase of applied uniaxial stress at the higher temperatures, 160–200°C, always resulted in an irreversible decrease in the measured resistivity. For example, increase in applied uniaxial stress from 110 to 170 MPa (25,000 psi) at 200°C resulted in a 20% decrease in the measured resistivity for a Pb-containing material with $x = 0.65$. However, the measured temperature dependence of the resistivity, $\Delta\rho(T)$, was not dependent on the applied uniaxial stress provided that the applied stress was kept constant. Thus, the precompaction and preheating procedures just described ensured the reproducibility of $\rho$ vs $T$ at a fixed sample compaction.

## Results and Discussion

### $\rho$ *versus* $T$ *for* $Pb_2Ru_2O_{6.5}$ *and* $Bi_2Ru_2O_7$

The measurement procedure just described was first applied to metal oxide powders for which conductivity versus temperature data were available in the literature either for sintered samples or for single crystals. The result for the resistivity versus temperature behavior for nonexpanded ($x = 0$) lead ruthenate, $Pb_2Ru_2O_{6.5}$, given in Fig. 3 shows metallic behavior similar to that previously reported for a sintered sample (*6*). The room temperature resistivity for the pressed powder sample is $(1.17 \pm 0.02) \times 10^{-3}$ ohm-cm as compared with $(0.27 \pm 0.1) \times 10^{-3}$ ohm-cm for a sintered polycrystalline sample (*6*). The

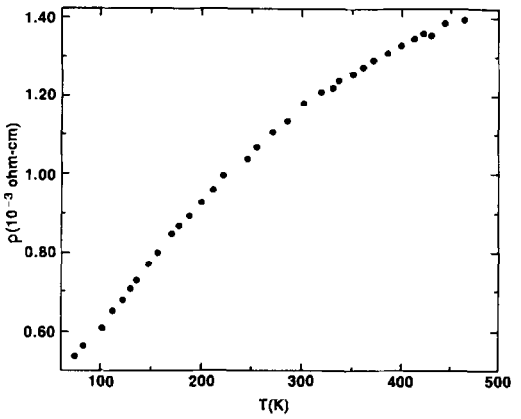


FIG. 3. Resistivity vs temperature for $Pb_2Ru_2O_{6.5}$.

ratio of the resistivity at room temperature to that at liquid $N_2$ temperature is $\rho(298\ K)/\rho(77\ K) = 2.2$ for our pressed powder sample as compared with $\rho(298\ K)/\rho(77\ K) = 3.0$ for a sintered sample (*6*). The resistivity versus temperature behavior for a pressed powder sample of stoichiometric bismuth ruthenate, $Bi_2Ru_2O_7$, is given in Fig. 4 and is compared with measurements by Bouchard and Gillson (*8*) on a sintered bar. For the temperature range 77 K $< T <$ 440 K the general features of the temperature dependence appear to agree fairly well except that the present work indicates a resistivity plateau for $T \sim 170$ K rather than a resistivity maximum at $T \sim 170$ K (*8*). The value $\rho(300\ K) = 2.85 \times 10^{-3}$ ohm-cm for this work is to be compared with $\rho(300\ K) = 0.70 \times 10^{-3}$ ohm-cm from measurements on a sintered bar (*8*). The effective density of the pressed powder samples of $Pb_2Ru_2O_{6.5}$ and $Bi_2Ru_2O_7$ was about 70% of the X-ray density, 8.9 g/cm$^3$.

The room temperature resistivities of pressed powder polycrystalline samples of $Pb_2Ru_2O_{6.5}$ and $Bi_2Ru_2O_7$ are about four times greater than those reported for well-sintered specimens (*6*, *8*). This discrepancy is probably due to the lower sample bulk density and associated problems of particle–particle contact in the pressed powders versus the sintered specimens. Since the electrical properties of polycrystalline bulk samples are highly dependent on sample preparation techniques, only measurements on pure single crystals can be considered accurate indications of the true resistivity. However, the general features of the temperature dependence of the resistivities of the pressed powder samples are similar to those for the well-sintered specimens. This indicates that the measurement techniques just described can be used to establish reliably the conductivity trends in the expanded ($x > 0$) pyrochlore compounds.

### *ρ versus T for* $Pb_2[Ru_{2-x}Pb_x]O_{6.5}$

The electrical resistivity versus temperature data for lead ruthenates within the composition range $0 \leq x \leq 1.06$ and for temperatures in the range 77 to 480 K are plotted in Fig. 5. It is evident that the expanded lead ruthenates are low-resistivity materials ($10^{-3}$ ohm-cm $< \rho < 10^{-1}$ ohm-cm) which exhibit a smooth variation from a positive to a negative temperature coefficient of resistivity with increasing Pb content. Materials with low Pb substitution

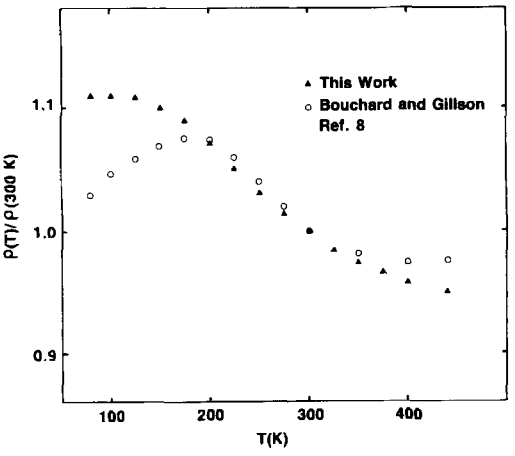


FIG. 4. Resistivity vs temperature for $Bi_2Ru_2O_7$. Comparison with measurements by Bouchard and Gillson (Ref. (*8*)) on a sintered bar.

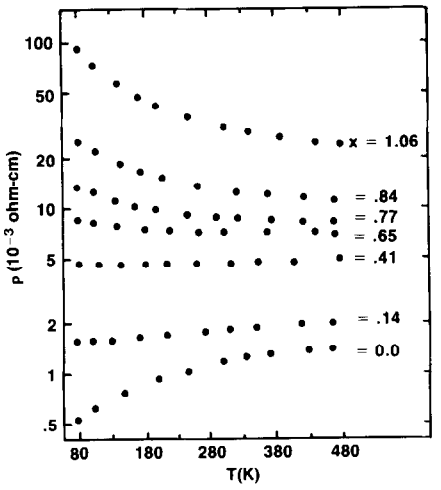


FIG. 5. Resistivity vs temperature for expanded lead ruthenate $Pb_2[Ru_{2-x}Pb_x]O_{6.5}$ for $0 \leq x \leq 1.06$.

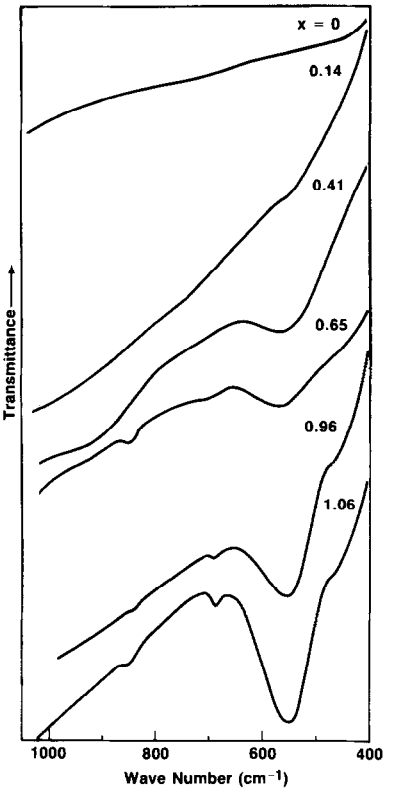


FIG. 6. Infrared absorption data for $Pb_2[Ru_{2-x}Pb_x]O_{6.5}$ for $0 \leq x \leq 1.06$.

show metallic-like behavior with a resistivity that increases with temperature. As Pb substitution is increased beyond $x \sim 0.4$ these materials show semiconducting-like behavior and a resistivity which decreases with increasing temperature. The change from metallic to semiconducting-like resistivity behavior with increasing Pb substitution, $x$, is also reflected in the infrared absorption results given in Fig. 6 for $0 \leq x \leq 1.06$. The materials with $x = 0$ and $x = 0.14$ show a continuous absorption characteristic of a high concentration of free electrons as in a metal, while the spectra for the materials with Pb substitution levels $x \geq 0.4$ show the development of a broad absorption band at about 550 $cm^{-1}$ with increasing Pb substitution. Similar observations have been reported for Ru-containing perovskite polytypes as a function of $3d$ transition metal ion substitution (*11*).

Upon replotting the resistivity data versus $1/T$ (Fig. 7) in order to obtain thermal activation energies $E_A$, where $E_A$ is defined by $\rho = \rho_0 \exp(E_A/kT)$, a maximum value of $E_A = 0.018$ eV is found for the most expanded material with $x = 1.06$. Although this behavior is reminiscent of a semiconductor with impurities in the band gap, these thermal activation energies are

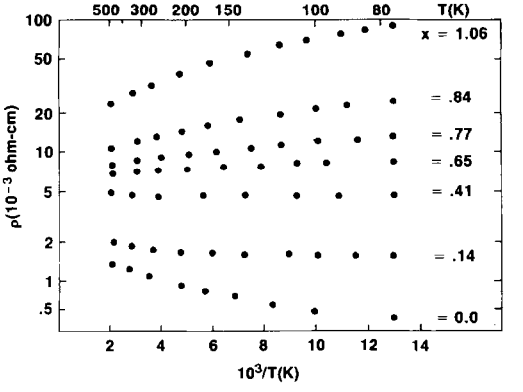


FIG. 7. Resistivity vs $1/T$ for $Pb_2[Ru_{2-x}Pb_x]O_{6.5}$ for $0 \leq x \leq 1.06$.

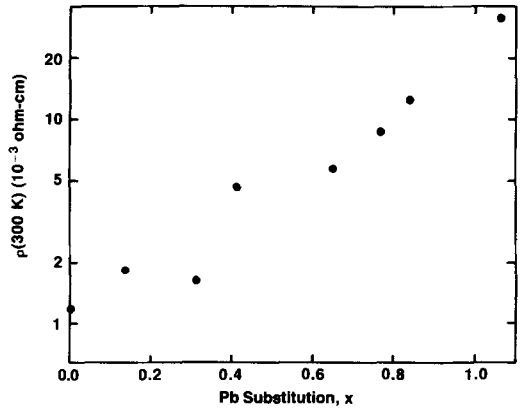


FIG. 8. Resistivity at 300 K vs Pb substitution, $x$, in $Pb_2[Ru_{2-x}Pb_x]O_{6.5}$.

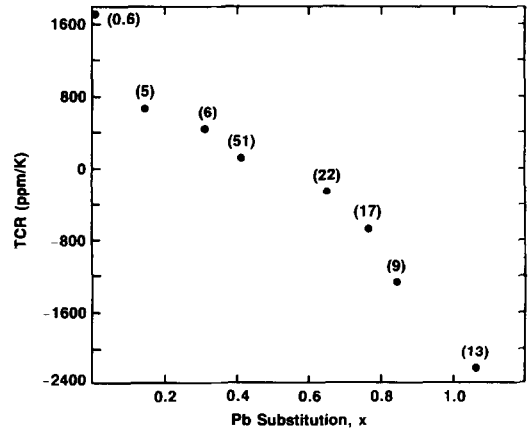


FIG. 9. Temperature coefficient of resistivity, TCR = $(1/\rho)(\Delta\rho/\Delta T)$, vs Pb substitution, $x$, in the vicinity of 300 K. The BET surface area value ($m^2/g$) for each composition is given in parentheses beside each data point.

too low to be characteristic of semiconductor or insulator dopant levels in metal oxides.

A plot of the resistivity versus Pb substitution (Fig. 8) and a plot of the temperature coefficient of resistivity (TCR = $(1/\rho)(\Delta\rho/\Delta T)$ versus Pb substitution (Fig. 9), each at 300 K, provide a further demonstration of the strong influence of composition on the resistivity behavior of these materials. There is a nearly linear increase in the magnitude of ln $\rho$(300 K) with Pb substitution (Fig. 8). There is a smooth decrease of the TCR with Pb substitution from about +1700 ppm for $x = 0$ to −2200 ppm at $x = 1.06$ as shown in Fig. 9. Here the BET surface area value in $m^2/g$ for each composition is given in parentheses beside each data point. Although surface areas ranged from 5 to 50 $m^2/g$, these data show that there is no systematic correlation between TCRs and changes in particle size associated with these large changes in surface area. For the samples with low Pb substitution, which showed metallic behavior, the TCRs plotted in Fig. 9 were determined from linear $\rho$ versus $T$ plots. Those samples with $x > 0.65$ showed large negative TCRs. In these cases the TCRs were determined from the ln $\rho$ versus $1/T$ plots making use of the fact that TCR = $d \ln \rho/dT = -(E_A/kT)(1/T)$. A summary of the resistivity and the temperature coefficient of resistivity values at selected temperatures for the Pb-substituted materials is given in Table II.

### $\rho$ *versus* $T$ *for* $Bi_2[Ru_{2-x}Bi_x]O_{7-y}$

Resistivity versus temperature data for $Bi_2[Ru_{2-x}Bi_x]O_{7-y}$ with three different compositions ($x$ = 0.0, 0.28, and 0.52) are

TABLE II

SELECTED RESISTIVITY AND TEMPERATURE COEFFICIENT OF RESISTIVITY VALUES FOR $Pb_2[Ru_{2-x}Pb_x]O_{6.5}$

| Pb substitution on $B$ site, $x$ | Resistivity, $\rho(10^{-3}$ ohm-cm) 200 K | 300 K | 400 K | TCR at 300 K (ppm/K) |
|---|---|---|---|---|
| 0 | 0.925 | 1.17 | 1.325 | +1710 |
| 0.14 | 1.696 | 1.82 | 1.93 | +670 |
| 0.31 | 1.58 | 1.64 | 1.73 | +437 |
| 0.41 | 4.65 | 4.70 | 4.77 | +120 |
| 0.65 | 6.08 | 5.76 | 5.65 | −260 |
| 0.765 | 9.62 | 8.65 | 8.18 | −680 |
| 0.84 | 15.27 | 12.80 | 11.52 | −1290 |
| 1.06 | 41.8 | 31.3 | 26.0 | −2260 |

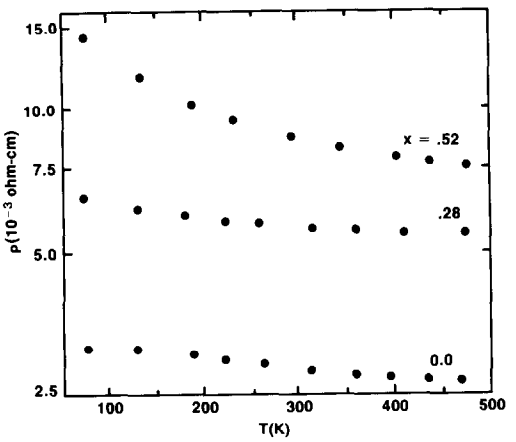


FIG. 10. Resistivity vs temperature data for expanded bismuth ruthenate, $Bi_2[Ru_{2-x}Bi_x]O_{7-y}$ for $x$ = 0.0, 0.28, and 0.52.

TABLE III

SELECTED RESISTIVITY AND TEMPERATURE COEFFICIENT OF RESISTIVITY VALUES FOR $Bi_2[Ru_{2-x}Bi_x]O_7$

| Pb substitution on $B$ site, $x$ | Resistivity, $\rho(10^{-3}$ ohm-cm) 200 K | 300 K | 400 K | TCR at 300 K (ppm/K) |
|---|---|---|---|---|
| 0 | 3.05 | 2.84 | 2.73 | −550 |
| 0.28 | 5.87 | 5.60 | 5.49 | −330 |
| 0.52 | 10.0 | 8.60 | 7.90 | −1160 |

presented in Fig. 10 and in Table III. As the extent of Bi substitution on the $B$ site is increased, the negative TCR becomes more pronounced, similar to the case for the Pb-substituted pyrochlores (Fig. 5 and 7). For comparable levels of substitution on the $B$ site, the Bi-substituted pyrochlores show somewhat higher resistivity and more negative TCRs than do the Pb-substituted pyrochlores (Tables II and III). In contrast to the case for the Pb-substituted materials, the Bi-substituted compounds do not show metallic-like behavior with positive TCRs, even at the lowest levels of substitution.

*Influence of Crystallinity on ρ versus T*

Two $Pb_2[Ru_{2-x}Pb_x]O_{6.5}$ samples, one with $x$ = 0.31 and one with $x$ = 0.77, were chosen for a study of the influence of crystallinity on the resistivity behavior. Both samples were prepared as X-ray-amorphous solids from alkaline solution by the methods previously described (*1, 2*). The resulting "incipient" pyrochlores were dried overnight at 100°C and measured. For each sample a subsequent resistivity measurement was performed after establishing crystallinity by heat treatment at 400°C. The results, at varying stages of crystallinity, are given in Figs. 11 and 12a for the $x$ = 0.31 and the $x$ = 0.77 pyrochlores. In Fig. 12b, the X-ray diffraction patterns for the $x$ = 0.77 compound are given for the incipient

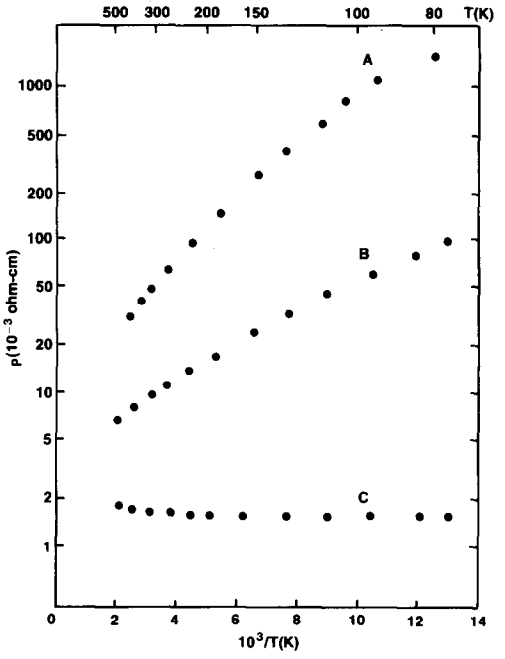


FIG. 11. Resistivity vs temperature for $Pb_2[Ru_{1.69}Pb_{0.31}]O_{6.5}$ at three stages of crystallinity. Data for incipient pyrochlore as prepared from solution (curve A); sample heat treated in compression cell at 250°C for 2 hr (curve B); sample heat treated overnight at 400°C (curve C).

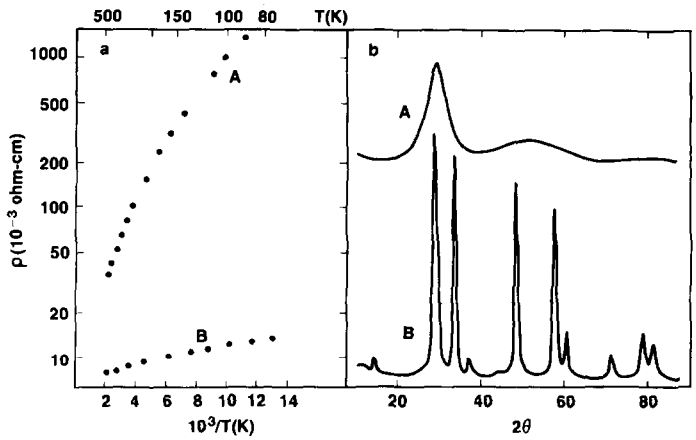


FIG. 12. (a) Resistivity vs temperature for $Pb_2[Ru_{1.23}Pb_{0.77}]O_{6.5}$. Incipient pyrochlore as prepared from solution (curve A); fully developed pyrochlore heat treated at 400°C (curve B). (b) X-ray patterns for the incipient pyrochlore (A) and for the crystalline material (B).

pyrochlore and for the fully developed pyrochlore showing the development of crystallinity after heat treatment at 400°C. For each composition, the incipient pyrochlore as prepared from solution shows a strong negative temperature characteristic with $E_A \approx 0.06$ eV as determined from the slope of the ln $\rho$ versus $1/T$ plots (curve A in Figs. 11 and 12a). Evidently, the resistivity behavior of the incipient (disordered) pyrochlores is not influenced by composition. An intermediate stage of development of long range order is represented by resistivity curve B in Fig. 11 for the $x = 0.31$ pyrochlore which was heat treated at 250°C for $2\frac{1}{2}$ hr in the compression cell and then remeasured. Here the negative temperature characteristic is less pronounced and $E_A \sim 0.025$ eV. For materials with fully developed crystallinity, the influence of composition is once again apparent. Curve C (Fig. 11) for the $x = 0.31$ pyrochlore shows metallic-like behavior and a small positive TCR, while the comparable resistivity plot for the $x = 0.77$ pyrochlore (curve B, Fig. 12a) shows a marked negative temperature characteristic with $E_A \sim 0.005$ eV. In both cases the conductivity is markedly increased as long range order develops, the increase being a factor of 32 for the $x = 0.31$ compound and a factor of 9 for the $x = 0.77$ compound at $T = 300$ K. A summary of the resistivity results for these two samples of expanded lead ruthenate at varying stages of crystallinity is given in Table IV.

## Conclusions

Electrical conductivity in the nonexpanded pyrochlore $Pb_2Ru_2O_{6.5}$ has been discussed previously (*6*). The conductivity mechanism in this oxide pyrochlore is believed to be rather closely related to that in perovskite transition metal oxides such as $SrRuO_3$ (*12*) that exhibit metallic behavior. It has been suggested that the $t_{2g}$ levels of the $Ru^{4+}$ ion are delocalized into a partially filled $\pi^*$ band (*12, 13*) resulting from covalent interaction with suitably directed oxygen orbitals. Since the $RuO_6$ octahedra in the perovskite $SrRuO_3$ are linked in a corner-shared three-dimensionally connected network, bulk conductivity results. By analogy, it is suggested that metallic conductivity in the

TABLE IV

MATERIALS AND RESISTIVITY DATA FOR $Pb_2[Ru_{2-x}Pb_x]O_{6.5}$ AT VARYING STAGES OF CRYSTALLINE DEVELOPMENT

| Sample No. | Composition $x$ | Preparation method (Ref. (1)) | BET surface area ($m^2/g$) | $\rho$ at 300 K ($10^{-3}$ ohm-cm) | $E_A$[a] (eV) | TCR at 300 K (ppm/K) |
|---|---|---|---|---|---|---|
| 1 | 0.31 | Amorphous from solution, 100°C, ON[b] air | 31 | 52.7 | 0.059 | −7540 |
| 2 | 0.31 | Sample 1, heated in compression cell, 250°C, 2½ hr, air | — | 10.3 | 0.025 | −3290 |
| 3 | 0.31 | Sample 1, 500°C, ON, air | 6 | 1.64 | — | +437 |
| 4 | 0.77 | Amorphous from solution, 100°C, ON, air | 54 | 78.0 | 0.060 | −7740 |
| 5 | 0.77 | Sample 4, 400°C, ON, air | 17 | 8.64 | 0.005 | −680 |

[a] $E_A$ is defined by $\rho = \rho_0 \exp(E_A/kT)$.
[b] ON = overnight.

pyrochlore $Pb_2Ru_2O_{6.5}$, which also contains a three-dimensionally connected network of $RuO_6$ octahedra, results predominantly from Ru–O interactions as in the case of $SrRuO_3$ (*6, 12*). While the conductivity mechanism discussed here may also be invoked to explain the high conductivity exhibited by $Bi_2Ru_2O_7$, Bouchard and Gillson (*8*) have pointed out that, to be consistent, any such model must also account for the fact that the rare earth ruthenates, such as $Eu_2Ru_2O_7$, are semiconducting. It was further suggested that conductivity does take place via Ru–O band states, but changes occur in the width or splittings of these states as a function of the *A* ion (*8*). Results of recent band structure calculations (*14*) support this view.

For those expanded pyrochlores which show a negative TCR and a thermally activated conductivity behavior, infrared absorption measurements (*15*) show only one strong band in the 500 to 800-$cm^{-1}$ region, a characteristic broad band at about 550 $cm^{-1}$ (see e.g., Fig. 6). This band has been assigned to Pb–O (or Bi–O) activity (*15*). The fact that Ru–O modes are either very weak or absent indicates that the Ru electrons are delocalized and that electrical conductivity takes place via Ru–O band states. We propose a qualitative picture for the electrical conductivity behavior exhibited by the Pb-substituted and the Bi-substituted pyrochlores involving percolation of the electrons among the connected networks of $RuO_6$ octahedra. The discussion which follows is developed specifically for the case of the Pb-based pyrochlores.

The presence of $Pb^{4+}$, which has no electrons to give up to the conduction band, is expected to cause a break in the –Ru–O–Ru–O– conduction pathways. The local effect of each $Pb^{4+}$, which is a considerably larger cation than $Ru^{4+}$, might well extend to surrounding lattice sites. For this reason the continued breakup of –Ru–O–Ru–O– conduction paths leads to thermally activated conductivity behavior at $x \gtrsim 0.5$ (Figs. 7 and 9), a substitution level lower than would be expected from standard percolation models (*16*). This hopping conductivity behavior is probably associated with electron transfer between large conducting segments, as contrasted with thermal activation of carriers from a valence band or impurity level into a conduction band as in a semiconductor. If this picture is correct, at sufficiently low temperatures ($T < 10$ K)

the thermal activation of carriers across the small insulating gaps introduced by substitution of $Pb^{4+}$ for Ru will diminish and resistivity will become independent of temperature as described by Sheng (*17*). Such a measurement was not possible using our apparatus owing to the large heat leaks associated with the technique for maintaining dynamic load during the measurement.

For the incipient or amorphous pyrochlores, the extent of the conducting pathways is governed by a characteristic short range order and not by the degree of Pb substitution. Accordingly, two incipient pyrochlores with widely different Pb substitution, $x = 0.31$ and $x = 0.77$, show the same large $E_A \sim 0.06$ eV (Table IV, Figs. 11 and 12). The incipient pyrochlores also show active modes associated with Pb–O but not with Ru–O bonds in infrared absorption measurements (*15*), suggesting that the short range order in these disordered materials encompasses clusters of corner-shared $RuO_6$ octahedra with delocalized electrons.

The smooth variation of the TCR for the Pb-substituted pyrochlores from positive to negative values with increasing Pb content (Figs. 7 and 9) suggests the application of these materials in the fabrication of electrical resistor compositions. The substitution of approximately 20% of the ruthenium by lead results in a material with essentially temperature-independent resistivity. The use of precious-metal-containing pyrochlores as resistor compositions is well established (*18–20*), but the Pb-substituted pyrochlores appear to have the advantages of economy and a "tailorable" TCR. However, the limited temperature stability of these variable stoichiometry pyrochlore compounds (*1*) may render many of these compositions incompatible with standard conditions for fabrication of thick-film resistors. In any case, the low-temperature synthesis route, which is applicable both to substituted and non-substituted compounds (*1, 2*), leads to small particle size and thereby allows the conducting threshold to be achieved at lower critical volume concentrations of the conductive oxide (*21*).

## Acknowledgments

The authors express their gratitude to Arlene Bloemeke-Strege for considerable assistance in data-taking and data-reduction, to Joe Lewandowski for much of the sample preparation, and to Harry Brady for obtaining thermogravimetric and X-ray diffraction results. We also thank Dr. Ken Poeppelmeier and Dr. John Steger for many helpful discussions, and we thank Dr. Steger for providing us with his powder conductivity cell, which served as the basis for our own conductivity cell design.

The authors also acknowledge Dr. R. J. Bouchard for pointing out the defect concentration dependencies inherent to standard percolation models.

## References

1. H. S. Horowitz, J. M. Longo, and J. T. Lewandowski, *Mater. Res. Bull.* **16,** 489 (1981).
2. H. S. Horowitz, J. M. Longo, H. H. Horowitz, and J. T. Lewandowski *in* "Solid State Chemistry in Catalysis" (R. K. Grasselli and J. F. Brazdil, Eds.), ACS Symposium Series 279, p. 143, Amer. Chem. Soc., Washington, DC (1985).
3. H. S. Horowitz, J. M. Longo, and H. H. Horowitz, *J. Electrochem. Soc.* **130,** 1851 (1983).
4. H. H. Horowitz, H. S. Horowitz, and J. M. Longo, *in* "Proceedings, Symposium on Electrocatalysis" (W. E. O'Grady, P. N. Ross, and F. G. Will, Eds.), Vol. 82-2, Electrochemical Soc., Pennington, NJ (1982).
5. A. W. Sleight, *Inorg. Chem.* **7,** 1704 (1968).
6. J. M. Longo, P. M. Raccah, and J. B. Goodenough, *Mater. Res. Bull.* **4,** 191 (1969).
7. R. A. Beyerlein, H. S. Horowitz, J. M. Longo, M. E. Leonowicz, J. D. Jorgensen, and F. J. Rotella, *J. Solid State Chem.* **51,** 253 (1984).
8. R. J. Bouchard and J. L. Gillson, *Mater. Res. Bull.* **6,** 669 (1971).
9. Karl-Joachim Euler, *J. Power Sources* **3,** 117 (1978).
10. Mykroy Ceramics Co., Orben Drive, Ledgewood, NJ 07852.

*11.* H. U. SCHALLER, A. EHMANN, AND S. KEMMLER-SACK, *Mater. Res. Bull.* **19,** 517 (1984).
*12.* J. M. LONGO, P. M. RACCAH, AND J. B. GOODENOUGH, *J. Appl. Phys.* **39,** 1327 (1968).
*13.* J. B. GOODENOUGH, *Bull. Soc. Chim. Fr.* **4,** 1200 (1965).
*14.* R. V. KASWOSKI, W. Y. HSU, A. W. SLEIGHT, A. L. WACHS, A. P. SHAPIRO, T.-C. CHIANG, AND M.-H. TSAI, *in* "Proceedings, 7th International Conference on Ternary and Multinary Compounds," p. 533, Materials Research Society, Pittsburgh, PA (1987).
*15.* R. A. BEYERLEIN AND H. S. HOROWITZ, to be published.
*16.* (a) H. SCHER AND R. ZALLEN, *J. Chem. Phys.* **53,** 3759 (1970); (b) I. DALBERG AND N. BINENBAUM, *Phys. Rev.* **B35,** 8749 (1987).
*17.* P. SHENG, *Phys. Rev. B* **21,** 2180 (1980).
*18.* G. E. PIKE AND C. H. SEAGER, *J. Appl. Phys.* **48,** 5152 (1977).
*19.* R. J. BOUCHARD, U.S. Patent 3,583,931 (1971).
*20.* P. R. VAN LOAN, U.S. Patent 3,682,840 (1972).
*21.* P. F. CARCIA, A. FERRETTI, AND A. SUNA, *J. Appl. Phys.* **53,** 5282 (1982).